J. Phys. Chem. Solids, 1977, Vol. 38, pp. 719–725. Pergamon Press. Printed in Great Britain

ON THE MAGNETIC PROPERTIES OF TRANSITION METAL SUBSTITUTED MnAs

KARI SELTE and ARNE KJEKSHUS
Kjemisk Institutt, Universitetet i Oslo, Blindern, Oslo 3, Norway

ARNE F. ANDRESEN
Institutt for Atomenergi, 2007 Kjeller, Norway
and

ANDRZEJ ZIĘBA
Institute of Nuclear Physics and Techniques, Academy of Mining and Metallurgy, 30-059 Kraków, Poland

(*Received* 1 *September* 1976; *accepted* 15 *October* 1976)

Abstract—The properties of $Mn_{1-t}T_tAs$ phases (T: V, Cr, Fe or Co; $0 < t \leqq 0.10$) are studied in external magnetic fields up to 250 kOe, and temperatures between 80 and 400 K. The results are presented and discussed in terms of phase diagrams comprising concentration, temperature, and magnetic field axes.

1. INTRODUCTION

Manganese mono-arsenide may be classified as one of the most intriguing compounds of inorganic chemistry. This statement is based on the peculiar transformational properties which, over the years, have been unveiled for this compound. Figure 1 summarizes certain aspects of the behaviour of MnAs as a function of temperature. The fact that its crystal structure at atmospheric pressure is of the NiAs type both at high and low temperatures, separated by an intermediate region of MnP type structure, is emphasized in the central portion of the diagram.

A more complete and varied picture of this peculiarity emerges from the right hand side of the diagram, where, according to Menyuk *et al.*[1], the structure type is shown as a function of pressure and temperature. An additional feature brought out in this temperature vs pressure equilibrium diagram is that MnAs may be (partly) converted back to MnP type structure below ~150 K.

Chemical substitution of other elements for Mn or As arises as a convenient alternative and supplement to pressure variation. Although the effect of small substitutions of P or Sb for As has been explored to some extent[2–5], attention is in the left hand side of Fig. 1 concentrated on the more systematically studied $Mn_{1-t}T_tAs$ phases (T hitherto: V, Cr, Fe or Co;[6–10]). Replacement of T for Mn in these phases leads to contraction of the unit cell, and the effect of substitution is accordingly to simulate compression. It should be noted that the two approaches are not equivalent, since chemical substitution also includes a change in the number of electrons per formula unit.

The two sides of Fig. 1 are seen to be in conformity. Extrapolation of the curves for T_N (Néel temperature) from both sides of the diagram leads to $T_N \approx 210$ K for a

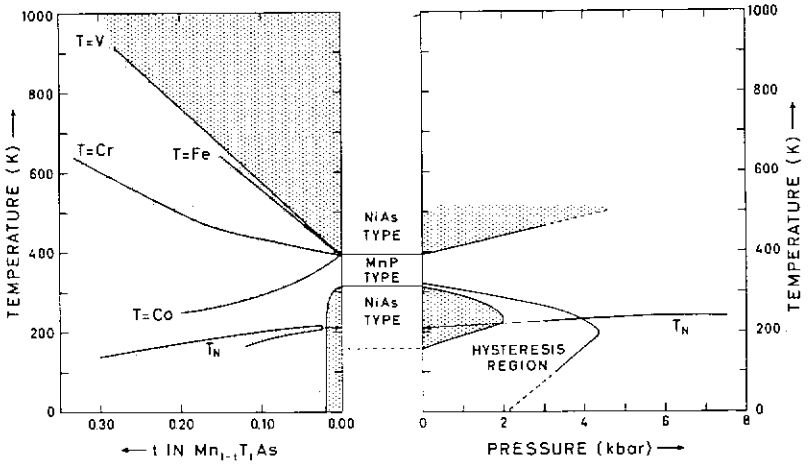

Fig. 1. Composite diagram showing temperature variation of structural properties of MnAs as functions of pressure and substitutional solid solution according to t of formula $Mn_{1-t}T_tAs$ (T: V, Cr, Fe or Co). Open shading denotes regions where NiAs type structure prevails and denser shading ranges of transition temperatures which depend on composition and specific T element. Data from [1, 6–10].

hypothetical helimagnetic mode of MnP type MnAs, as opposed to its real ferromagnetic NiAs type state with $T_C \approx 315$ K[11]. This observation together with the fact that the helimagnetic mode in $Mn_{1-t}T_tAs$ (T = V, Cr, Fe or Co) is of the double, a-axis type (see [7–10]) and not of the double, c-axis type[12, 13] found in a number of other phases with MnP type structure, suggest very strongly that the magnetic mode is depending on the overall as well as the detailed atomic arrangement.

The object of the present study has been to examine structural and magnetic changes in $Mn_{1-t}T_tAs$ phases imposed by applied, variable magnetic fields (H), i.e. to introduce the latter as a third variable parameter on the left hand side of Fig. 1.

2. EXPERIMENTAL

Batches of VAs, CrAs, MnAs, FeAs and CoAs were prepared from the elements (99.5% V (A. D. Mackay), 99.5% Cr (Koch-Light Laboratories; crushed powder from commercial, electrolytic grade material), 99.9+% Mn (The British Drug Houses; crushed powder from commercial, electrolytic grade material), 99.99% Fe and 99.99+% Co (Johnson, Matthey & Co; turnings from rods) and 99.9999% As (Koch-Light Laboratories)) using the sealed silica capsule technique. Ternary samples were subsequently made by heating desired proportions (MnAs with 1, 3, 5 or 10% TAs (T: V, Cr, Fe or Co) substitution) of the binary compounds according to the procedures in [7–10]. The homogeneity, composition and structural state of the samples at room temperature were ascertained from powder X-ray (Guinier) diffraction photographs.

Measurements in strong magnetic fields (up to ~250 kOe) were performed with a pulsed magnetometer of essentially conventional design[14] at temperatures between 80 and 350 K. The pulsed magnetic field was obtained by discharging condensors (3000 μF, 3 kV) connected with a pulsed solenoid through a thyristor switch. The solenoid, comprising the magnetometer sensor inside, was cooled by liquid nitrogen. The pulsed signals were observed on an oscilloscope screen and registered photographically. The background signals for no sample positioned inside the solenoid were measured separately and used to correct the (100–200 mg) sample signal. A Cu-constantan thermocouple localized inside the sample was used for temperature measurements. Data reduction (to $M(H)$ and $dM(H)/dH$) was performed numerically on an ODRA 1304 computer. Relative errors in H and M are estimated to be ~3 and ~6%, respectively.

The pulsed magnetometer was also used to determine Curie temperatures. The weak, sinusoidal field utilized for this purpose was obtained by supplying the solenoid from a sound generator and the signal was measured by means of a sensitive microvoltmeter.

Magnetization and susceptibility measurements in weak magnetic fields (1.2–12 kOe) were carried out with a Foner type magnetometer and by the Faraday method.

3. PROPERTIES IN WEAK MAGNETIC FIELDS

As summarized in Fig. 2 there is a clearcut distinction between the low temperature, weak field magnetic behaviours of $Mn_{1-t}V_tAs$ samples with $t \leqq 0.03$ and

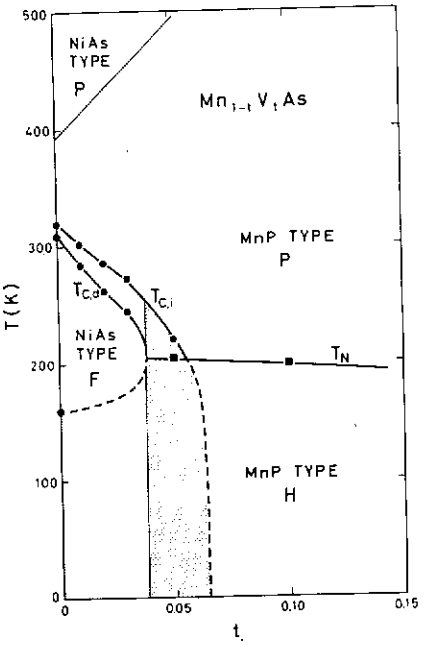

Fig. 2. Temperature variation of some structural and magnetic properties of $Mn_{1-t}V_tAs$ as function of t. Open shading denotes region where ferromagnetic (F) state only comes up in high fields and denser shading region where helimagnetic (H) state only can be obtained by application of external pressure.

$0.03 < t \leqq 0.10$. Near room temperature MnAs and the Mn rich $Mn_{1-t}T_tAs$ samples exhibit first order phase transitions, with hysteresis, between ferromagnetic and paramagnetic states, and the data for $Mn_{0.99}Fe_{0.01}As$ in Fig. 3 may serve as an example of this. The Curie temperatures for increasing ($T_{C,i}$) and decreasing ($T_{C,d}$) temperature are given in Table 1, together with values for the ferromagnetic moment (μ_F). $T_{C,i}$, $T_{C,d}$ and μ_F decrease with increasing t whereas the area of the hysteresis loop is found to increase. The results in Fig. 4 for $Mn_{1-t}T_tAs$ ($0.03 < t \leqq 0.10$) may be interpreted as reflecting transformations between paramagnetic and antiferromagnetic states at the cusps on the curves. Both sets of data can be more clearly understood when the knowledge[6–10] of structural and magnetic properties in the absence of external magnetic fields is taken into

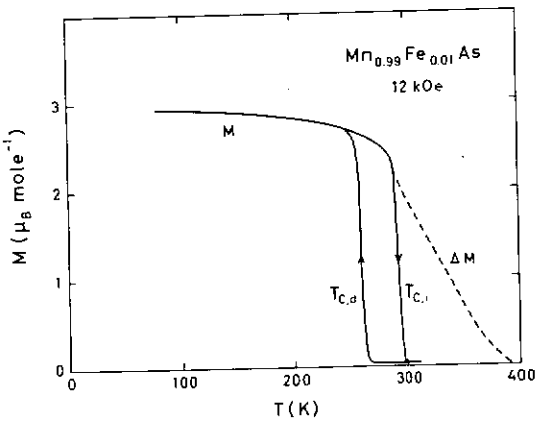

Fig. 3. Magnetization vs temperature for $Mn_{0.99}Fe_{0.01}As$ at 12 kOe (solid curves) and magnetization increment at the metamagnetic transition above T_C (broken curve).

Table 1. Magnetic moments and critical magnetic fields and temperatures for $Mn_{1-t}T_tAs$ ($0 \leqq t \leqq 0.10$); last digits uncertain

		MnP type state				NiAs type state		
T	t	T_N(K)	H_C (kOe) max. value	H_S (kOe) at 80 K	μ_S (μ_B) at $H > H_S$	$T_{C,i}$ (K)	$T_{C,d}$ (K)	$\mu_F(\mu_B)$ at 80 K, 12 kOe
V	0.01	—	—	—	—	303	283	3.0
	0.02	—	—	—	—	285	261	2.9
	0.03	—	—	—	—	276	245	1.85
	0.05	203	70	~180	1.4	220	—	1.6
	0.10	197	55	~150	1.27	—	—	—
Cr	0.01	—	—	—	—	316	287	3.02
	0.03	—	—	—	—	302	281	2.58
	0.05	—	—	—	—	~285	~253	0.33
	0.10	211	60	83	1.55	—	—	—
Fe	0.01	—	—	—	—	291	260	2.97
	0.03	216	70	~85	1.6	—	—	—
	0.05	213	56	~60	1.4	—	—	—
	0.10	201	37	~40	1.25	—	—	—
Co	0.01	—	—	—	—	310	294	2.9
	0.03	—	—	—	—	274	247	2.7
	0.05	197	87	>250	—	222	—	2.0
—	0.00	—	—	—	—	317	306	3.07

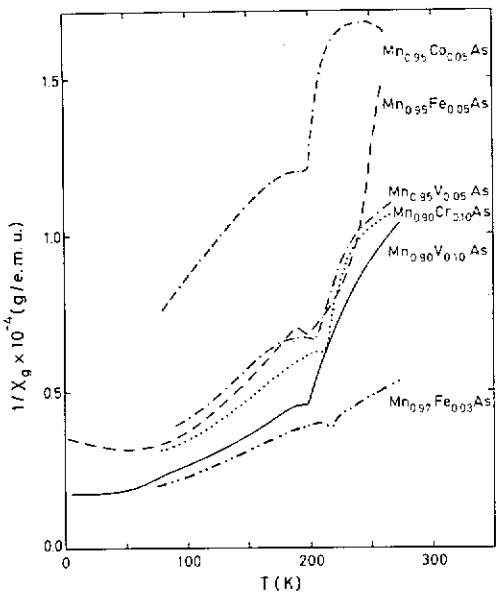

Fig. 4. Reciprocal magnetic susceptibility as function of temperature for typical $Mn_{1-t}T_tAs$ samples ($0.03 < t \leqq 0.10$).

account. The distinction arises because not only two different types of cooperative magnetism are involved, but also two different types of atomic arrangement.

As brought out already in Fig. 1, the ferromagnetic mode of MnAs with NiAs type structure extends slightly into the ternary regions of $Mn_{1-t}T_tAs$. The ferromagnetic moments and Curie temperatures given in Table 1 are slightly lower than those for pure MnAs[1]. The paramagnetic moments and θ-values stay virtually constant at $\mu_P = \sqrt{(8C_{mol})} = 4.5 \pm 0.3\,\mu_B$ and $\theta = 270 \pm 10$ K on going from MnAs to the ternary samples. Neglecting the distinction between μ_F- and μ_P-values, the cooperative mode in $Mn_{1-t}T_tAs$ ($0 \leqq t < \sim 0.05$) may be referred to as a kind of high spin state. Since the ferromagnetic mode occurs already in weak or zero external magnetic fields, no further information is expected on turning to stronger external fields.

For samples with $t \geqq 0.05$ for T = V or Co, $t \geqq 0.03$ for T = Fe and $t \geqq 0.10$ for T = Cr in $Mn_{1-t}T_tAs$ the transition at T_N (see Fig. 4 and Table 1) in weak or zero field occurs between paramagnetic and helimagnetic states of the MnP type atomic arrangement. This inference is based on neutron diffraction investigations[7–10] in zero field, which consistently show a double, a axis (the MnP type cell arranged according to $Pnma$; $c > a > b$) spiral structure. The values for T_N, as determined from the local minima in $1/\chi$(T) curves (Table 1), agree with those given in [7–10]. Values for the magnetic moment cannot be estimated from susceptibility data of the non-Curie–Weiss law type shown in Fig. 4. However, on turning to strong fields and low temperatures such values are obtained as saturation moments (μ_S), which are given in Table 1 together with the saturation field (H_S). These saturation moments agree rather well with those (μ_H) derived by neutron diffraction[7–10] for the helimagnetic states in zero applied field. On comparing μ_H or μ_S with μ_P or μ_F for samples with an NiAs type atomic arrangement, the label "low spin state" for samples with MnP type structure appears to be justified.

From qualitative band theory considerations magnetic moments between 1 and 2 μ_B have been predicted[1,2] for the "low spin state" and moments between 3 and 4 μ_B for the "high spin state" of MnAs. Thus, the moments observed for the "low spin state" are in good agreement with the predictions, whereas the "high spin moments" are lower than expected.

4. PROPERTIES IN STRONG MAGNETIC FIELDS

In Fig. 5 is shown the magnetization curves ($M(H)$) for $Mn_{0.95}Fe_{0.05}As$ at selected temperatures as typical example of the results obtained in strong magnetic fields for all samples. The interpretation of this band of curves is achieved on the basis of the knowledge about the behaviour of the same sample in weak or zero external magnetic fields.

At temperatures below T_N the helimagnetic state is stable in the absence of external magnetic fields. Hence, the $M(H)$ curves in Fig. 5(a) reflect reversible transitions from an initial, helimagnetic to a final, ferromagnetic state. Since the magnetic moment remains essentially unchanged throughout this process, it is inferred that no structural transformation is involved. A more careful analysis of the curves (see the corresponding derivative curves in Fig. 5(b)) unveils that the apparently continuous transitions are composed of two resolvable characteristics, *viz*, two critical fields exist, one corresponding to a transition between a normal and conically deformed helimagnetic mode in comparatively weak field (H_C) and the other to the completion of the conical deformation to a ferromagnetic mode at H_S. Since the investigated samples were polycrystalline, a more detailed analysis of the $M(H)$ curves is unfortunately not possible.

As seen from Table 1 the magnitude of H_C is similar (37–87 kOe) for the various $Mn_{1-t}T_tAs$ samples with some variation with T, t and T. The situation is quite different for H_S which varies appreciably in magnitude as well as in functional dependence on T, t and T. H_S is, for example, relatively small for T = Fe and particularly large for T = Co where saturation was not obtained even at 250 kOe. H_S has always its highest value near T_N and decreases rapidly with decreasing temperature.

For the helimagnetic $Mn_{1-t}T_tAs$ samples with small amounts of T, a strong magnetic field can induce a magneto-structural transition to a ferromagnetic, NiAs type state. This kind of irreversible transition to ferromagnetism in strong fields has earlier been detected by Galkin *et al.*[15, 16] for $Mn_{0.97}Co_{0.03}As$ and $Mn_{0.98}Fe_{0.02}As$, and is here also observed for $Mn_{0.95}V_{0.05}As$ and $Mn_{0.95}V_{0.05}As$.

The $M(H)$ curves for $Mn_{0.95}V_{0.05}As$ are given in Fig. 6, where at low temperatures (85, 120 and 150 K) only reversible, hysteresisless transitions are seen. However, at 190 and 240 K the magnetization and demagnetization curves are separated by large hystereses and the magnetic moment changes by a factor of nearly two. At 240 K the hysteresis loop is closed, whereas at 190 K the demagnetization leads to a permanent ferromagnetic state when the external field is brought back to zero. Clearly, the transition is of first order between a paramagnetic MnP type and a ferromagnetic NiAs type state. This behaviour is observed in a narrow temperature interval below ~208 K for $Mn_{0.95}V_{0.05}As$ (~220 K for $Mn_{0.95}Co_{0.05}As$). These strong field induced NiAs,F type states are maintained for an indefinite period of time in zero field when $T < T_{C,i}$, whereas heating above the Curie temperature restores the stable zero field situation. The Curie temperatures $T_{C,i}$ and the magnetic moments for these samples in the metastable state are listed in Table 1.

The results are conveniently rationalized in temperature vs applied magnetic field phase diagrams, a selection being presented in Figs. 7–10. If H is regarded as a third coordinate axis perpendicular to t and T in Fig. 1, each of the individual diagrams of Figs. 7–10 can

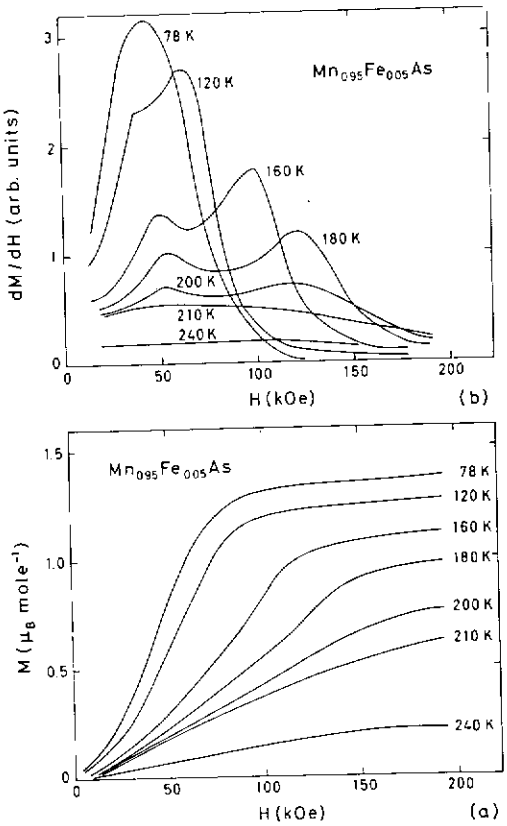

Fig. 5. Magnetization vs applied field at different temperatures for $Mn_{0.95}Fe_{0.05}As$ (a); corresponding derivative curves (b).

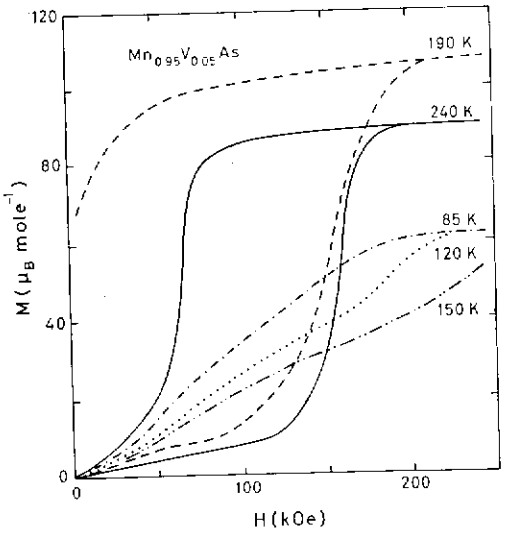

Fig. 6. Magnetization as function of applied field at various temperatures for $Mn_{0.95}V_{0.05}As$.

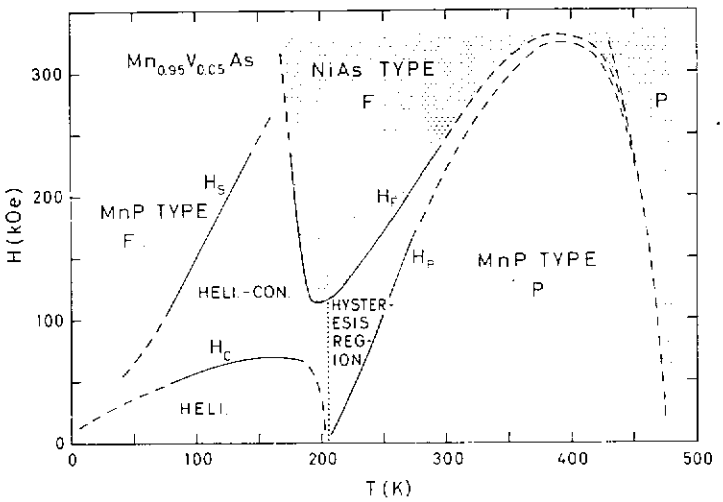

Fig. 7. Phase diagram in T,H space for $Mn_{0.95}V_{0.05}As$.

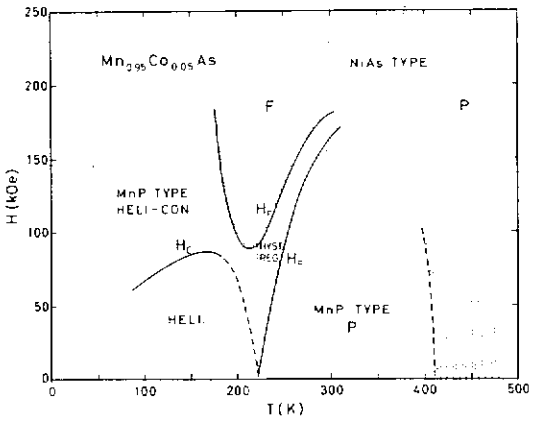

Fig. 8. Phase diagram in T,H space for $Mn_{0.95}Co_{0.05}As$.

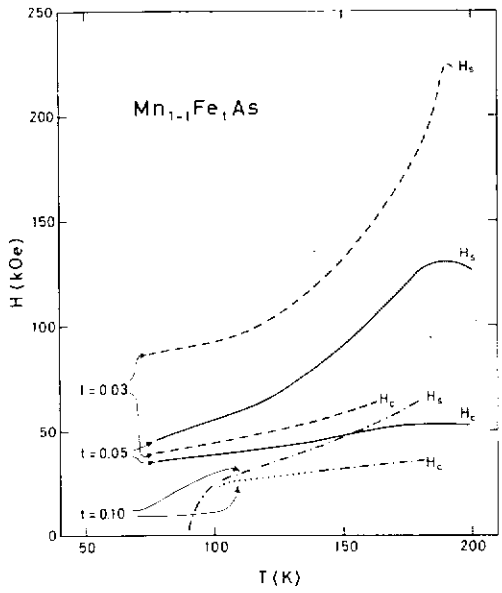

Fig. 9. Low temperature portion of T,H phase diagram for $Mn_{1-t}Fe_tAs$.

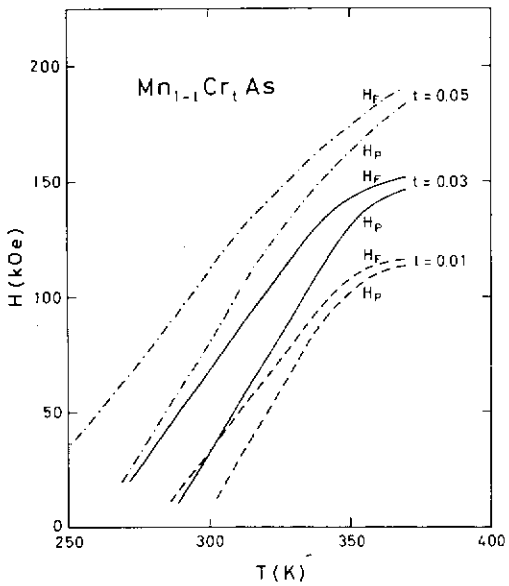

Fig. 10. High temperature portion of T,H phase diagram for $Mn_{1-t}Cr_tAs$.

be looked upon as a section of constant t through t, T, H space.

The data for $Mn_{0.95}V_{0.05}As$ in Fig. 7 will be used as a specific example in the following considerations, and the changes which become evident on comparison with Figs. 8–10 may serve to illustrate variations with the substituent (T) and its concentration (t). As seen from Figs. 7 and 8 the change from T = V to Co affects mainly the phase borders at the low temperature side of the diagram, and it is particularly worthwhile to denote that the H_S-curve in Fig. 8 is shifted to $H > 250$ kOe (*vide supra*). The variation in H_S as well as H_C with t for a given T is shown in Fig. 9 for $Mn_{1-t}Fe_tAs$. The data for $Mn_{1-t}Cr_tAs$ in Fig. 10 are presented to expose changes in the high temperature portion of these T, H diagrams with t.

Returning to Fig. 7 for $Mn_{0.95}V_{0.05}As$, the ex-

perimentally determined phase borders are represented by solid curves, and the hypothetical extrapolations of these are given as broken curves. The unshaded and shaded areas represent regions with MnP and NiAs type structures, respectively. The extrapolated border between these structure types from ~300 to 485 K[8] is positioned on the basis of our findings for MnAs[17].

The transitions of the types MnP,$P \leftrightarrows$NiAs,P, NiAs,$P \leftrightarrows$NiAs,F, MnP,heli.$\leftrightarrows$MnP,heli.-con., MnP,-heli.-con.$\leftrightarrows$MnP,F are reversible and either of a crystallographic or magnetic nature, whereas MnP,$P \rightarrow$ NiAs,F and MnP,heli.-con.$\rightarrow$NiAs,F involve structural as well as magnetic changes. The MnP,$P \rightarrow$NiAs,F type transition is seen to be quasi-reversible over the range 208–~310 K, where the transition in increasing and decreasing fields is separated by a hysteresis loop ($H_F > H_P$). The quasi-reversible situation persists until $H_P = 0$ at 208 K, below which temperature the H_F-curve has no counterpart to govern an NiAs,$F \rightarrow$MnP,heli.-con. type transition. In accordance with this, the $Mn_{0.95}V_{0.05}As$ sample undergoes incomplete hysteresis loops for $\sim 170 < T < 208$ K (see the $M(H)$ curves for 190 K in Fig. 6). Hence, on carrying such a sample through a magnetization ($H > H_F$)-demagnetization cycle in this temperature interval a ferromagnetic state will be irreversibly induced. The lowest value for the transition field H_F (114 kOe) is observed in the vicinity of T_N = 203 K for $Mn_{0.95}V_{0.05}As$. According to data in Table 1 and Figs. 7 and 8 the irreversible, field induced ferromagnetism in $Mn_{1-t}T_tAs$ occurs over a narrow composition range in which $T_{C,i} > T_N$ and the extrapolated value for $T_{C,d} < T_N$.

5. MAGNETOCALORIMETRIC EFFECT

An additional advantage of pulsed field magnetic measurements is that this technique allows the detection of changes in sample temperature (ΔT) arising from the influence of the applied field, ΔT was measured as an ephemeral voltage signal from the thermocouple inside the sample. Due to the good thermal contact between the sample and the environment, the measured ΔT will consistently come out smaller than expected.

A reversible magnetization-demagnetization cycle leads to no change in internal energy of the sample. However, if the cycle is associated with a hysteresis, the net magnetic work applied on the sample (proportional to $\oint M(H)\,dH$) is dissipated as heat, leading to $\Delta T \neq 0$ under adiabatic conditions. When the final state is different from the initial, a temperature change arises as a result of their energy difference.

Figure 11 shows the magnetocalorimetric data for $Mn_{0.95}V_{0.05}As$ in the temperature interval 170–270 K as obtained by 210 kOe pulsed magnetic field. These data provide a further support for the phase diagram in Fig. 7. Thus, for $T > \sim 260$ K, $H_F > 210$ kOe and consequently $\Delta T = 0$ K as observed. For $\sim 208 < T < \sim 260$ K the ΔT vs T curve reflects the reversible MnP,$P \leftrightarrows$NiAs,F transition, the increase in ΔT with decreasing T being consistent with increased area of the hysteresis loop. On the assumption that the specific heat of $Mn_{0.95}V_{0.05}As$ approximates that of MnAs[18] (above T_C) a calculated

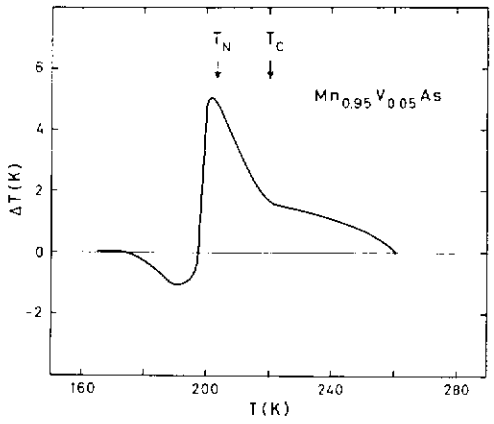

Fig. 11. Change in sample temperature caused by 210 kOe pulsed magnetic field as function of temperature for $Mn_{0.95}V_{0.05}As$.

value of 1.5 K for ΔT is obtained from $M(H)$ at 240 K (Fig. 6), in good conformity with the value given in Fig. 11. In the region $\sim 200 < T < \sim 208$ K where the irreversible MnP,heli.$\rightarrow$NiAs,F transition occurs, an appreciable increase in ΔT is observed, the positive ΔT implying that the final NiAs,F state has the lowest energy. Hence, this is not the result of work on the sample by the magnetic field, but may be determined by local inhomogeneities in composition, temperature etc. of the sample. The influence of this effect ceases at ~200 K, where a rapid decrease in the ΔT vs T curve is seen. The negative position of the $\Delta T(T)$ curve between ~195 and ~170 K is consistent with the fact that the internal energy of the MnP,heli. state is lower than that of the NiAs,F state. For $T < \sim 170$ K again $H_F > 210$ kOe, and consequently $\Delta T = 0$ K.

Acknowledgements—The authors are grateful to T. Zalewski and Z. Oburszko for help in the magnetization measurements, and to R. Troć for magnetic susceptibility measurements at liquid helium temperature. This work has received financial support from *The Norwegian Research Council for Science and the Humanities*.

REFERENCES

1. Menyuk N., Kafalas J. A., Dwight K. and Goodenough J. B., *Phys. Rev.* **177**, 942 (1969).
2. Goodenough J. B., Ridgley D. H. and Newman W. A., *Proceedings of the International Conference on Magnetism*, p. 542. Nottingham (1964).
3. Ido H., *J. Phys. Soc. Japan* **25**, 1543 (1968).
4. Hall E. L., Schwartz L. H., Felcher G. P. and Ridgley D. H., *J. Appl. Phys.* **41**, 939 (1970).
5. Schwartz L. H., Hall E. L. and Felcher G. P., *J. Appl. Phys.* **42**, 1621 (1971).
6. Kazama N. and Watanabe H., *J. Phys. Soc. Japan* **30**, 1319 (1971).
7. Selte K., Kjekshus A. and Andresen A. F., *Acta Chem. Scand.* **A28**, 61 (1974).
8. Selte K., Kjekshus A., Valde G. and Andresen A. F., *Acta Chem. Scand.* **A30**, 8 (1976).
9. Selte K., Kjekshus A., Valde G. and Andresen A. F., *Acta Chem. Scand.* **A30**, 468 (1976).
10. Selte K., Kjekshus A. and Andresen A. F., to be published.
11. Bacon G. E. and Street R., *Nature* **175**, 518 (1955).
12. Felcher G. P., *J. Appl. Phys.* **37**, 1056 (1966).
13. Forsyth J. B., Pickart S. J. and Brown P. J., *Proc. Phys. Soc.* **88**, 333 (1966).

14. Nizioł S., Zięba A. and Kulka J., *Zeszyty Naukowa AGH* **483**, 63 (1975) (in polish).
15. Galkin A. A., Savadskii E. A., Smirnov V. M. and Valkov V. A., *Proceedings of the International Conference on Magnetism*, p. 508, Moscow (1973); *Sov. Phys.—Doklady* **19**, 593 (1975).
16. Galkin A. A., Savadskii E. A., Smirnov V. M. and Valkov V. A., *Sov. Phys.—JETP Letters* **20**, 253 (1974).
17. Selte K., Kjekshus A., Andresen A. F. and Zięba A., to be published.
18. Grønvold F., Snildal S. and Westrum E. F., *Acta Chem. Scand.* **24**, 285 (1970).